Letter

Mitigating the fermion sign problem by automatic differentiation

Zhou-Quan Wan,[1] Shi-Xin Zhang,[1,*] and Hong Yao[1,2,†]
[1]*Institute for Advanced Study, Tsinghua University, Beijing 100084, China*
[2]*State Key Laboratory of Low Dimensional Quantum Physics, Tsinghua University, Beijing 100084, China*

(Received 11 October 2020; revised 21 November 2022; accepted 22 November 2022; published 20 December 2022)

As an *intrinsically unbiased* method, the quantum Monte Carlo (QMC) method is of unique importance in simulating interacting quantum systems. Although the QMC method often suffers from the notorious sign problem, the sign problem of quantum models may be mitigated by finding better choices of the simulation scheme. However, a general framework for identifying optimal QMC schemes has been lacking. Here, we propose a general framework using automatic differentiation to automatically search for the best QMC scheme within a given ansatz of the Hubbard-Stratonovich transformation, which we call "automatic differentiable sign optimization" (ADSO). We apply the ADSO framework to the honeycomb lattice Hubbard model with Rashba spin-orbit coupling and demonstrate that ADSO is remarkably effective in mitigating and even solving its sign problem. Specifically, ADSO finds a sign-free point in the model which was previously thought to be sign-problematic. For the sign-free model discovered by ADSO, its ground state is shown by sign-free QMC simulations to possess spiral magnetic ordering; we also obtained the critical exponents characterizing the magnetic quantum phase transition.

DOI: 10.1103/PhysRevB.106.L241109

Introduction. The numerical study of quantum systems is of vital importance, especially in the context of strongly correlated systems which are in general analytically intractable in more than one dimension. Due to their exponentially growing Hilbert space, numeric methods such as exact diagonalization usually fail when the system size is moderately large. The quantum Monte Carlo (QMC) method can putatively overcome such an "exponential wall" by sampling a fraction of the Hilbert space stochastically. The QMC method is *intrinsically unbiased*, making it one of the most powerful and successful methods to simulate quantum systems. Unfortunately, the QMC method is often plagued by the notorious sign problem when dealing with fermion systems or frustrated spin models [1–3]. When the sign problem occurs, the simulation uncertainty increases exponentially with the system size and inverse temperature, rendering it infeasible in studying systems at low temperature or with large size [4–10]. It has been desired for decades to solve the sign problem of interacting quantum models.

Tremendous progress has been made to solve the sign problem by identifying sign-free QMC schemes for quantum models with certain symmetries [11–15] (see, e.g., Ref. [16] for a recent review). In studying these fermion models by the sign-problem-free QMC method, fruitful physics has been revealed (see, e.g., Refs. [17–53]). Nonetheless, *generically* solving the sign problem of quantum models is almost impossible as it has been proved that the sign problem complexity is NP-hard [54]. Moreover, it was shown recently that interacting models whose ground states feature certain properties such as a gravitational anomaly may have an intrinsic sign problem [55–58]. Fortunately, for a given *specific* quantum model it is still possible to solve or mitigate its sign problem. Efforts in this direction have been made recently; sign problem mitigation was studied using basis transformation [59–65], Lefschetz thimbles [66–68], and machine learning techniques [69–71]. However, a universal framework for solving or mitigating the sign problem is still lacking.

Here, we fill in this gap by constructing a general framework of sign optimization in the determinant quantum Monte Carlo (DQMC) method. The DQMC method was introduced by Blankenbecler, Scalapino, and Sugar (BSS) [72] and has been extensively used in simulating interacting fermion models. Note that the severity of the sign problem in the DQMC method crucially depends on the scheme of Hubbard-Stratonovich (HS) transformation. Different forms of HS transformations were proposed in the early stages of developing the DQMC method [5,73–77]. Nonetheless, previous HS transformations employed in simulations are quite limited in form and are constrained to *no* spatial dependence. It is desired to construct sufficiently general HS transformations and then find the optimized one for the sign of a given model. In this Research Letter, we propose a general framework to realize sign optimization by parametrizing HS transforms continuously and optimizing the sign using automatic differentiation (AD) [78–80]. We call it "automatic differentiable sign optimization" (ADSO). (AD is a powerful method for optimization that is widely encountered in machine learning and features various applications in computational physics [81–90].) ADSO is a general framework for mitigating the sign problem, applicable to most quantum lattice fermion models. We believe that ADSO will shed light on the nature of the sign problem.

*zsx16@mails.tsinghua.edu.cn
†yaohong@tsinghua.edu.cn

We further demonstrate the effectiveness of the general ADSO framework by applying it to the Rashba-Hubbard model (the usual Hubbard model plus Rashba couplings) on a honeycomb lattice. Although the Rashba-Hubbard model at half filling was known to be sign-problematic [91], we show that its sign problem can be significantly mitigated by ADSO, which leads power-law acceleration. More remarkably, with the assistance of ADSO, we find a sign-free point in the model. This leads to an exponential acceleration in simulations and allows one to reliably obtain its physical properties by the sign-free QMC method. For the sign-free model identified by ADSO, its ground state is shown by large-scale QMC simulations to possess spiral magnetic ordering (as shown in Fig. 3 below). We further obtained critical exponents characterizing the quantum phase transition between the Dirac semimetal at weak Hubbard interaction and the spiral magnetic ordered state at strong interaction.

The DQMC method and the sign problem. The DQMC method is widely used in simulating interacting fermion models. To study equilibrium properties of an interacting fermion model described by Hamiltonian $\hat{H} = \hat{H}_0 + \hat{H}_I$ with $\hat{H}_0$ being the noninteracting term and $\hat{H}_I$ being the quartic or interacting term, one normally computes the expectation value of some observable $\hat{O}$: $\langle\hat{O}\rangle = \frac{\mathrm{Tr}(\hat{O}e^{-\beta\hat{H}})}{\mathrm{Tr}(e^{-\beta\hat{H}})}$, where $\beta = 1/T$ is the inverse temperature. Using the Suzuki-Trotter decomposition [92,93] along the imaginary time direction, we obtain the density matrix $e^{-\beta\hat{H}} = \prod_{l=0}^{L-1} e^{-\Delta\tau\hat{H}} \simeq \prod_{l=0}^{L-1} e^{-\Delta\tau\hat{H}_0} e^{-\Delta\tau\hat{H}_I}$, where $\beta = L\Delta\tau$. To deal with the quartic term $\hat{H}_I$, one can convert it into quadratic forms by performing HS transformations; the price to pay is the introduction of auxiliary fields. A general form of HS transformation is given by

$$e^{-\Delta\tau\hat{H}_I} = \sum_s \eta(s) e^{\hat{V}(s)}, \tag{1}$$

where s represents auxiliary fields, $\hat{V}(s) = c^\dagger V(s) c$ are quadratic fermion operators with the matrix $V(s)$ and fermion creation operators $c^\dagger$ (indices in $c^\dagger$ are implicitly included), and $\eta(s)$ is a prefactor. For simplicity we assume that s take discrete values, though continuously valued auxiliary fields [94] can also be treated in ADSO. With HS transformation at every time slice l, we obtain the HS decoupled form of the density matrix: $e^{-\beta\hat{H}} = \sum_{\boldsymbol{s}} \prod_{l=0}^{L-1} \eta(s_l) e^{-\Delta\tau\hat{H}_0} e^{\hat{V}(s_l)} = \sum_{\boldsymbol{s}} \hat{\rho}_{\boldsymbol{s}}$, where $\boldsymbol{s} = \{s_l\}$ represent an auxiliary-field configuration.

Then, the expectation value of observable $\hat{O}$ is given by $\langle\hat{O}\rangle = \frac{\sum_{\boldsymbol{s}} w(\boldsymbol{s}) O(\boldsymbol{s})}{\sum_{\boldsymbol{s}} w(\boldsymbol{s})}$, where $O(\boldsymbol{s})$ is the expectation of $\hat{O}$ in the auxiliary-field configuration $\boldsymbol{s}$ and $w(\boldsymbol{s}) = \mathrm{Tr}(\hat{\rho}(\boldsymbol{s})) = \eta(\boldsymbol{s}) \det(\mathbb{I} + \prod_{l=0}^{L-1} e^K e^{V(s_l)})$ is the Boltzmann weight of auxiliary-field configuration $\boldsymbol{s}$ with K being the matrix obtained from $-\Delta\tau\hat{H}_0 = c^\dagger K c$ and $\eta(\boldsymbol{s}) = \prod_{l=0}^{L-1} \eta(s_l)$. To obtain $\langle\hat{O}\rangle$ by the QMC method, one computes the expectation of $O(\boldsymbol{s})$ with $\boldsymbol{s}$ sampled from an un-normalized distribution $w(\boldsymbol{s})$, namely, $\langle\hat{O}\rangle = \langle O(\boldsymbol{s})\rangle_{\boldsymbol{s}\sim w(\boldsymbol{s})}$. However, there is no guarantee that $w(\boldsymbol{s})$ is always positive. When $w(\boldsymbol{s})$ can take both positive and negative (sometimes complex) values, we have the so-called sign problem.

When the sign problem appears, the absolute value of $w(\boldsymbol{s})$ can be used to sample the configurations by absorbing the sign or phase factor $e^{i\varphi(\boldsymbol{s})} = w(\boldsymbol{s})/|w(\boldsymbol{s})|$ into observables: $\langle O(\boldsymbol{s})\rangle_{\boldsymbol{s}\sim w(\boldsymbol{s})} = \frac{\langle e^{i\varphi(\boldsymbol{s})} O(\boldsymbol{s})\rangle_{\boldsymbol{s}\sim|w(\boldsymbol{s})|}}{\langle e^{i\varphi(\boldsymbol{s})}\rangle_{\boldsymbol{s}\sim|w(\boldsymbol{s})|}}$, where the denominator and numerator can be calculated stochastically using the Markov chain Monte Carlo method with the auxiliary fields sampled from the distribution $|w(\boldsymbol{s})|$. The denominator is the so-called average sign S in the QMC method: $S \equiv \langle e^{i\varphi(\boldsymbol{s})}\rangle_{\boldsymbol{s}\sim|w(\boldsymbol{s})|} = \frac{\sum_{\boldsymbol{s}} w(\boldsymbol{s})}{\sum_{\boldsymbol{s}} |w(\boldsymbol{s})|}$. As the partition function $Z = \mathrm{Tr}(e^{-\beta\hat{H}}) = \sum_{\boldsymbol{s}} w(\boldsymbol{s})$ is always positive, the average sign S must be positive, and it can be easily proved that $0 < S \leqslant 1$. It was observed [4] that the average sign decays exponentially with system size N and inverse temperature β as $S \sim e^{-\kappa N\beta}$ for sufficiently large N and β, where κ is a constant. For the sign-problematic (sign-free) QMC method, $\kappa > 0$ ($\kappa = 0$). When the sign problem occurs, to obtain the value of $\langle\hat{O}\rangle$ within a given accuracy, the needed QMC simulation time M increases exponentially with size and inverse temperature: $M \sim \frac{1}{S^2} \sim e^{2\kappa N\beta}$. This exponential complexity greatly hinders the feasibility of applying the QMC method to study interacting systems with large size or low temperature; reducing κ means sign mitigation and *power-law* acceleration. When the sign problem is solved (namely, what we have is sign-free), M is reduced to power-law complexity, $M \sim N^3\beta$; solving the sign problem represents *exponential* acceleration.

The ADSO framework. The average sign S or the prefactor κ discussed above is *not* an intrinsic property of a quantum model; instead it crucially depends on how the HS transformation is performed in the DQMC method. For a given model, a smaller κ implies a less severe sign problem. In other words, mitigating the sign problem is equivalent to reducing κ by identifying an optimal HS transformation. Suppose we have a set of possible HS transformations that can be parametrized by continuous parameters $\boldsymbol{\xi}$; the form of the HS transformation in Eq. (1) now becomes

$$e^{-\Delta\tau\hat{H}_I} = \sum_s \eta(\boldsymbol{\xi}, s) e^{\hat{V}(\boldsymbol{\xi},s)} = \sum_s \eta(\boldsymbol{\xi}, s) e^{c^\dagger V(\boldsymbol{\xi},s) c}. \tag{2}$$

Consequently, $w(\boldsymbol{\xi}, \boldsymbol{s}) = \eta(\boldsymbol{\xi}, \boldsymbol{s}) \det[\mathbb{I} + \prod_{l=0}^{L-1} e^K e^{V(\boldsymbol{\xi},s_l)}]$, $S(\boldsymbol{\xi})$, and $\kappa(\boldsymbol{\xi})$ can all depend on the HS parameters $\boldsymbol{\xi}$. Sign mitigation becomes an optimization problem in the parameter space of $\boldsymbol{\xi}$.

Here, we choose $\ln S$ instead of S as our objective function for optimization and would like to maximize $\ln S$ (equivalently maximizing S). We do not use S directly because it may lead to vanishingly small gradients due to the possible exponential smallness of S. Using the fact that the partition function Z of a given model is independent of $\boldsymbol{\xi}$, we obtain the differentiation of $\ln S$ as $d\ln S = -\mathrm{Re}\langle\frac{dw(\boldsymbol{\xi},\boldsymbol{s})}{w(\boldsymbol{\xi},\boldsymbol{s})}\rangle_{\boldsymbol{s}\sim|w(\boldsymbol{\xi},\boldsymbol{s})|}$ (see the Supplemental Material (SM) for details [95]). Note that sign averaging is not involved here, which means computing the gradients itself is actually *sign-free*. It is interesting that gradients of $\ln S$ could be efficiently and reliably calculated even though it is difficult to compute S accurately. Remarkably, the ADSO framework itself is sign-free; thus the ADSO framework can be directly applied on large-size systems of interest. See the SM for details [95] of computing the differentiation $\frac{dw(\boldsymbol{\xi},\boldsymbol{s})}{w(\boldsymbol{\xi},\boldsymbol{s})}$ using AD. It turns out that only very limited computational resources in addition to the standard DQMC algorithm are required in our ADSO framework.

Now we have all the ingredients to calculate the gradients. It is worth noting that we shall collect the gradients of many samples similar to previous methods of combining AD with Monte Carlo sampling [90,96,97]. Stochastic gradient descent (SGD) is suitable in our case to optimize the target function $\ln S$ since the gradients are calculated in a stochastic way: $\boldsymbol{\xi} \to \boldsymbol{\xi} + \delta \nabla_{\boldsymbol{\xi}} \ln S$, where δ is the learning rate.

The honeycomb Rashba-Hubbard model. We now apply our general ADSO framework to the honeycomb lattice Hubbard model with Rashba spin-orbit couplings [98]. The Hamiltonian of the honeycomb Rashba-Hubbard model at half filling is given by

$$\hat{H} = -t \sum_{\langle ij \rangle} c_{i\alpha}^{\dagger} c_{j\alpha} + \lambda_R \sum_{\langle ij \rangle} i\hat{z} \cdot (\boldsymbol{\sigma}_{\alpha\beta} \times \boldsymbol{d}_{ij}) c_{i\alpha}^{\dagger} c_{j\beta} + U \sum_i \left(n_{i\uparrow} - \frac{1}{2} \right) \left(n_{i\downarrow} - \frac{1}{2} \right), \tag{3}$$

where $c_{i\alpha}^{\dagger}$ creates an electron on site i with spin polarization $\alpha = \uparrow, \downarrow$, $n_{i\alpha} = c_{i\alpha}^{\dagger} c_{i\alpha}$, $\langle ij \rangle$ labels the nearest-neighbor (NN) sites i and j, $\boldsymbol{\sigma}$ represent Pauli matrices, and $\boldsymbol{d}_{ij}$ is the vector pointing from site i to site j. We set the hopping $t = 1$ as the energy unit. λ_R is the Rashba spin-orbit coupling, and U is the Hubbard interaction. This model is relevant to single-layer graphene on a substrate or an interface; for instance, the Rashba spin-orbit coupling has been observed in a graphene interface [99,100]. The model is invariant under the particle-hole transformation $c_{i\sigma} \to (-1)^i \sigma c_{i\bar{\sigma}}^{\dagger}$; it describes a system at half filling. This model is known to be sign-free only when $\lambda_R = 0$. For any $\lambda_R > 0$, this model was believed to be sign-problematic [91]. A natural question to ask is what HS transformation can give rise to the most mitigated and even solved sign problem for $\lambda_R > 0$.

For the repulsive Hubbard interaction, we consider a general HS transformation with the auxiliary fields on each site i coupled to spin operators along the direction $\boldsymbol{n}_i = (\sin\theta_i \sin\phi_i, \sin\theta_i \cos\phi_i, \cos\theta_i)$ with two continuous parameters θ_i and ϕ_i [77]:

$$e^{-\Delta\tau U (n_{i\uparrow} - \frac{1}{2})(n_{i\downarrow} - \frac{1}{2})} = \frac{1}{2} e^{-U\Delta\tau/4} \sum_{s_i = \pm 1} e^{\lambda s_i c_i^{\dagger} \boldsymbol{\sigma} \cdot \boldsymbol{n}_i c_i}, \tag{4}$$

where $\cosh\lambda = \exp(U\Delta\tau/2)$ and s_i is the auxiliary field. Since $s_i = \pm 1$, the HS parameters $\boldsymbol{n}_i$ feature the equivalence $\boldsymbol{n}_i \equiv -\boldsymbol{n}_i$; consequently, hereinafter we can assume $n_i^z \geqslant 0$ for any i. For repulsive Hubbard interactions, uniform $\boldsymbol{n}_i = \hat{z}$ for all i has been chosen conventionally. However, in trying to optimize for the best HS transformations, the ADSO framework will allow spatially nonuniform $\boldsymbol{n}_i$, which turns out to be crucial for mitigating or solving the sign problem of a model which was conventionally thought to be sign-problematic.

First, we apply ADSO to the Rashba-Hubbard model with $\lambda_R = 1.0$ and $U = 6.0$ to test the performance of the method. For the $3 \times 3 \times 2$ lattice and starting from randomly chosen $\boldsymbol{n}_i$, we found that the optimized $\boldsymbol{n}_i$ is not uniform spatially, namely, $\boldsymbol{n}_i = (0, 0.57, 0.82)$ for the $i \in A$ sublattice and $\boldsymbol{n}_i = (0, -0.57, 0.82)$ for the $i \in B$ sublattice as shown in the inset of Fig. 1(a). Inspired by the optimal pattern obtained for the small system, we constrain the HS transformations to $(\theta_i, \phi_i) = (\theta, 0)$ for the $i \in A$ sublattice and $(\theta_i, \phi_i) = (-\theta, 0)$ for the $i \in B$ sublattice, where $0 \leqslant \theta \leqslant \frac{\pi}{2}$ can vary to maximize the average sign. As shown in Fig. 1(a), we find that θ are converged to almost the same value for larger system sizes. This indicates that the optimized HS transformation does not change significantly with the system size; consequently, the optimized pattern obtained for relatively small system size can be directly used to perform QMC simulations on larger system size.

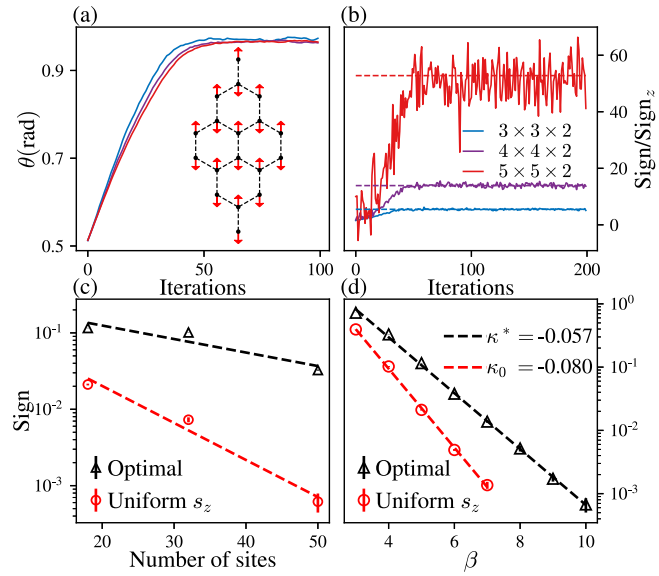

FIG. 1. Results of ADSO for the Rashba-Hubbard model on the honeycomb lattice with $\lambda_R = 1.0$ and $U = 6.0$. Here, we fix $\phi_i = 0$ and $\theta_{A,i} = -\theta_{B,i} = \theta$, which means θ is the only variational HS parameter. The corresponding pattern of $\boldsymbol{n}_i$ is shown in the inset of (a) (projected to the xy plane). Flow of HS parameters θ (a) and sign optimization results (b) for models with $3 \times 3 \times 2$, $4 \times 4 \times 2$, and $5 \times 5 \times 2$ lattice sites (periodic boundary condition). In each iteration, the gradient is averaged using 336×100 samples, where 336 is the number of parallel Markov chains. The optimized values of parameters θ are nearly the same for different system sizes. (c) The scaling of sign average S vs N; (d) the scaling of sign average S vs β.

Moreover, as shown in Fig. 1(b), the larger the system size is, the more the sign problem improves. This indicates that the optimized HS transformation can reduce the prefactor κ compared with the uniform $\boldsymbol{n}_i = \hat{z}$ scheme. Since the Monte Carlo (MC) computation time M scales as $M \sim \frac{1}{S^2} \sim e^{2\kappa N\beta}$, sign mitigation can be quantitatively characterized by how much the exponential prefactor κ is reduced from optimizing HS transformations. We use κ^* ($S^* \sim e^{-\kappa^* N\beta}$ and $M^* \sim e^{2\kappa^* N\beta}$) to denote its value in the optimized HS transformation scheme and κ_0 ($S_0 \sim e^{-\kappa_0 N\beta}$ and $M_0 \sim e^{2\kappa_0 N\beta}$) to denote the value in the spatially uniform HS scheme without optimization. Then, the computation is power-law accelerated from M_0 to $M^* \sim M_0^r$, where $r = \kappa^*/\kappa_0$. As shown in Figs. 1(c) and 1(d), by comparing the scaling of the average sign S versus β and N, between the previously used HS scheme and the ADSO optimized one, we obtain $r = \kappa^*/\kappa_0 \approx 0.7$. The power-law acceleration with $r \approx 0.7$ can lead to tremendous acceleration especially when the system is large or the temperature is

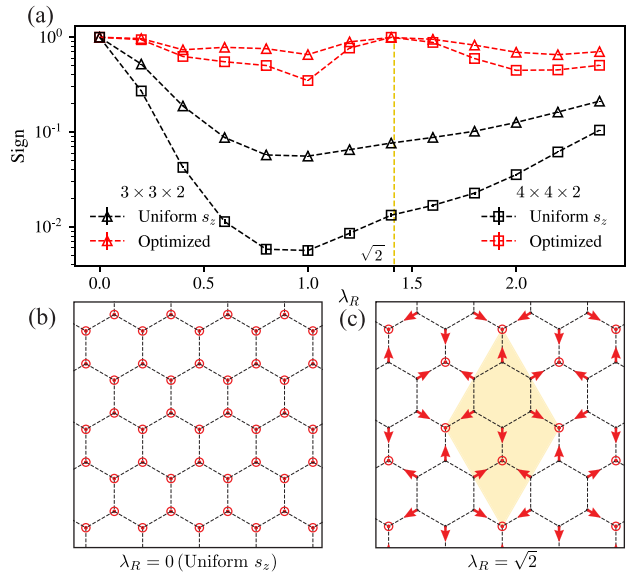

FIG. 2. Automatic sign optimization for the Rashba-Hubbard model with different parameters on the honeycomb lattice with $L = 3, 4$ (open boundary condition) and HS schemes for sign-free points. Here we choose $\beta = 5$, $U = 6$ and fix $t = 1$. (a) Optimized sign compared with the sign of the commonly used uniform s_z HS channel. (b) Sign-problem-free pattern of HS parameters $\boldsymbol{n}$ for the plain Hubbard model ($\lambda_R = 0$), where red $\odot$ represent that $\boldsymbol{n}$ is pointing in the $\hat{z}$ direction (it is indeed the uniform s_z channel). (c) Sign-problem-free pattern of HS parameters $\boldsymbol{n}$ for the Rashba-Hubbard model at $\lambda_R/t = \sqrt{2}$. Arrows represent the projection of $\boldsymbol{n}$ in the xy plane. As indicated by the shaded region, $\boldsymbol{n}$ manifest a periodicity of 2×2.

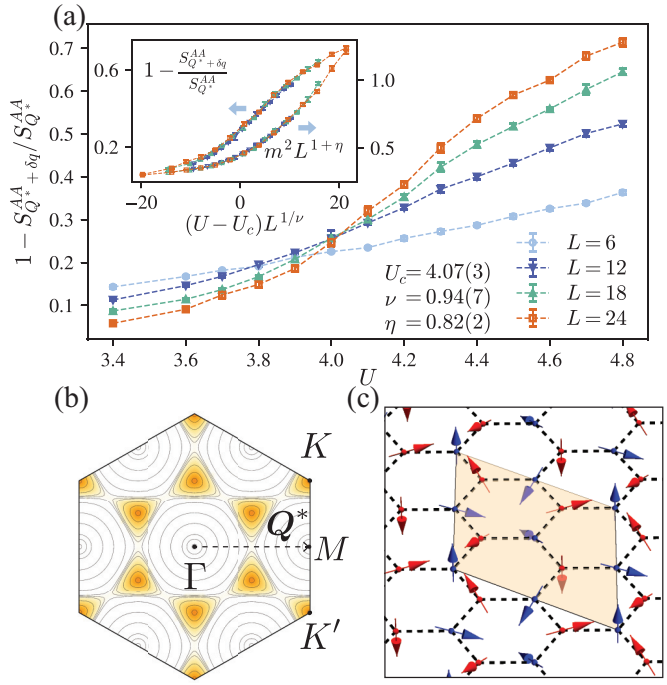

FIG. 3. The Rashba-Hubbard model at $\lambda_R/t = \sqrt{2}$. (a) Finite-size scaling of correlation ratio $R = 1 - S^{AA}_{\boldsymbol{Q}^*+\boldsymbol{\delta q}}/S^{AA}_{\boldsymbol{Q}^*}$, where $S^{AA}_{\boldsymbol{Q}}$ is the spin structure factor defined as $\frac{1}{L^2}\sum_{\boldsymbol{x}_1,\boldsymbol{x}_2} e^{i\boldsymbol{Q}\cdot(\boldsymbol{x}_1-\boldsymbol{x}_2)}\langle \boldsymbol{S}^A(\boldsymbol{x}_1)\cdot\boldsymbol{S}^A(\boldsymbol{x}_2)\rangle$, $\boldsymbol{Q}^* = \overline{\Gamma M}$, and $\boldsymbol{\delta q} = \boldsymbol{a}/L$ with $\boldsymbol{a}$ being the reciprocal lattice constant. Inset: Data collapse of R and $m^2 \equiv S^{AA}_{\boldsymbol{Q}^*}/L^2$ using the critical value U_c and the exponent ν, η extracted from the data of $L = 12, 18, 24$ using the method in Refs. [101,102]. Here we choose $\beta = L$ such that we can approach zero temperature in the thermodynamic limit. (b) Contour plot of single particle gap of the Rashba-Hubbard model with $U = 0$. It clearly shows eight two-component Dirac fermions in the Brillouin zone with two at the K, K' point and six in the middle of Γ-K, Γ-K'. (c) Visualization of magnetic order at $U > U_c$. This magnetic order manifests a periodicity of 2×2 as shown by the shaded region. (This visualization is based on spin-spin correlations in different directions; see SM for details [95].)

low. For instance, for the lattice with $N = 3 \times 3 \times 2 = 18$ sites and inverse temperature $\beta = 20.0$, the acceleration is already huge, and the computation is about $M_0/M^* \sim 10^7$ times faster.

The sign-free point identified by ADSO. We further apply the ADSO method to the honeycomb Rashba-Hubbard model for various values of λ_R, as shown in Fig. 2(a). It was previously known that the model is sign-free only for $\lambda_R = 0$ (fixing $t = 1$). For $\lambda_R = 0$, the sign-free HS transformation is successfully found by ADSO, and it is indeed a uniform $\boldsymbol{n}_i = \hat{z}$ pattern, as shown in Fig. 2(b). When λ_R is increased from zero to finite values, the optimized sign is shown as in Fig. 2(a). Surprisingly, we notice that for $\lambda_R = 1.4$ the average sign has been optimized to 0.996, which is very close to 1 (an average sign equal to 1 means that it is sign-free). The optimized sign being so close to 1 indicates that there may be an exactly sign-free point around this parameter region. Indeed, we find that $\lambda_R = \sqrt{2}$ is in fact an exactly sign-free point in the Rashba-Hubbard model using the HS transformation shown in Fig. 2(c) (see the SM for the exact proof [95]) and this sign-free point was clearly indicated from the ADSO optimized sign being extremely close to 1. This successful example of solving the sign problem implies that ADSO has the potential possibility of helping people notice or identify new sign-free models.

For the sign-free point $\lambda_R = \sqrt{2}$, we can perform large-scale QMC simulations to obtain reliably its quantum phase diagram as a function of U, as shown in Fig. 3(a). For $0 < U < U_c$, the ground state is a Dirac semimetal with *eight* Dirac points (two-component Dirac fermion) as shown in Fig. 3(b). For $U > U_c$, the ground state develops a spiral magnetic order as is shown in Fig. 3(c). This phase transition should belong to the $N_f = 16$ (using the convention in Ref. [43]) chiral Heisenberg Gross-Neveu-Yukawa (GNY) universality class [103]. From the finite-size scaling analysis of our QMC results, we obtain that the critical point is at $U_c = 4.07(3)$ with the correlation-length exponent $\nu = 0.94(7)$ (correlation length $\xi \sim |U - U_c|^{-\nu}$) and order-parameter anomalous dimension $\eta = 0.82(2)$. We highlight that these critical exponents of the $N_f = 16$ chiral Heisenberg GNY universality class are obtained from sign-free QMC simulations (QMC results of critical exponents of the Heisenberg GNY universality class in (2+1)D were obtained only with smaller N_f [43,51]).

As can be seen from the results above (both sign-mitigated and sign-solved cases), the optimized HS transformation, unlike the commonly used uniform $\boldsymbol{n}_i = \hat{z}$ decoupling scheme,

is not spatially uniform. The optimal pattern of $\boldsymbol{n}_i$ can be different for different model parameters, which may be related to the properties of its underlying spin correlations of the ground states; for the two sign-free cases ($\lambda_R = 0$ or $\lambda_R = \sqrt{2}$), the optimal patterns are indeed directly related to the magnetic ordering at strong U.

Discussion and concluding remarks. The general framework of mitigating the sign problem in the DQMC method proposed in this Research Letter can be used in principle in any interacting quantum lattice models as long as its HS transformation can be continuously parametrized. For instance, by enlarging the auxiliary-field space or allowing hybrid decoupling schemes, further sign optimization may be obtained (see the SM for details [95]). Moreover, the general idea of AD can be further applied to other types of QMC methods including world-line MC and hybrid MC whenever continuous parametrization can be implemented.

ADSO provides a general framework to mitigate the sign problem of interacting models; it worked remarkably well for the Rashba-Hubbard model which leads to power-law accelerations in general and even exponential acceleration for the sign-free point found here. It is desirable to apply ADSO in the future to other strongly correlated models whose solutions remain elusive so far. Moreover, ADSO has the potential possibility of identifying new sign-free models of interacting fermions.

Acknowledgments. We thank Steve Kivelson and Zheng-Zhi Wu for helpful discussions and especially Zi-Xiang Li for related collaborations. This work is supported in part by the NSFC under Grant No. 11825404 (S.-X.Z., Z.-Q.W., and H.Y.), the MOSTC under Grant No. 2021YFA1400100 and No. 2018YFA0305604 (H.Y.), and the Strategic Priority Research Program of Chinese Academy of Sciences under Grant No. XDB28000000 (H.Y.).

[1] J. E. Hirsch, Phys. Rev. B **31**, 4403 (1985).
[2] M. Takasu, S. Miyashita, and M. Suzuki, Prog. Theor. Phys. **75**, 1254 (1986).
[3] N. Hatano and M. Suzuki, Phys. Lett. A **163**, 246 (1992).
[4] E. Y. Loh, J. E. Gubernatis, R. T. Scalettar, S. R. White, D. J. Scalapino, and R. L. Sugar, Phys. Rev. B **41**, 9301 (1990).
[5] G. G. Batrouni and R. T. Scalettar, Phys. Rev. B **42**, 2282 (1990).
[6] F. F. Assaad and H. G. Evertz, in *Computational Many-Particle Physics*, Lecture Notes in Physics Vol. 739, edited by H. Fehske, R. Schneider, and A. Weiße (Springer, Berlin, 2008), pp. 277–356.
[7] C. J. Jia, E. A. Nowadnick, K. Wohlfeld, Y. F. Kung, C. C. Chen, S. Johnston, T. Tohyama, B. Moritz, and T. P. Devereaux, Nat. Commun. **5**, 3314 (2014).
[8] V. I. Iglovikov, E. Khatami, and R. T. Scalettar, Phys. Rev. B **92**, 045110 (2015).
[9] Y. F. Kung, C. C. Chen, Y. Wang, E. W. Huang, E. A. Nowadnick, B. Moritz, R. T. Scalettar, S. Johnston, and T. P. Devereaux, Phys. Rev. B **93**, 155166 (2016).
[10] E. W. Huang, C. B. Mendl, S. Liu, S. Johnston, H. C. Jiang, B. Moritz, and T. P. Devereaux, Science **358**, 1161 (2017).
[11] C. Wu and S. C. Zhang, Phys. Rev. B **71**, 155115 (2005).
[12] L. Wang, Y. H. Liu, M. Iazzi, M. Troyer, and G. Harcos, Phys. Rev. Lett. **115**, 250601 (2015).
[13] Z. X. Li, Y. F. Jiang, and H. Yao, Phys. Rev. B **91**, 241117(R) (2015).
[14] Z. X. Li, Y. F. Jiang, and H. Yao, Phys. Rev. Lett. **117**, 267002 (2016).
[15] Z. C. Wei, C. Wu, Y. Li, S. Zhang, and T. Xiang, Phys. Rev. Lett. **116**, 250601 (2016).
[16] Z. X. Li and H. Yao, Annu. Rev. Condens. Matter Phys. **10**, 337 (2019).
[17] S. Capponi and F. F. Assaad, Phys. Rev. B **63**, 155114 (2001).
[18] F. F. Assaad, Phys. Rev. B **71**, 075103 (2005).
[19] M. Hohenadler, T. C. Lang, and F. F. Assaad, Phys. Rev. Lett. **106**, 100403 (2011).
[20] K. Bouadim, Y. L. Loh, M. Randeria, and N. Trivedi, Nat. Phys. **7**, 884 (2011).
[21] E. Berg, M. A. Metlitski, and S. Sachdev, Science **338**, 1606 (2012).
[22] Z. Cai, H. H. Hung, L. Wang, and C. Wu, Phys. Rev. B **88**, 125108 (2013).
[23] D. Wang, Y. Li, Z. Cai, Z. Zhou, Y. Wang, and C. Wu, Phys. Rev. Lett. **112**, 156403 (2014).
[24] Z. X. Li, Y. F. Jiang, and H. Yao, New J. Phys. **17**, 085003 (2015).
[25] Y. Schattner, S. Lederer, S. A. Kivelson, and E. Berg, Phys. Rev. X **6**, 031028 (2016).
[26] Y. Schattner, M. H. Gerlach, S. Trebst, and E. Berg, Phys. Rev. Lett. **117**, 097002 (2016).
[27] Z. X. Li, F. Wang, H. Yao, and D. H. Lee, Sci. Bull. **61**, 925 (2016).
[28] F. F. Assaad and T. Grover, Phys. Rev. X **6**, 041049 (2016).
[29] Y. Y. He, H. Q. Wu, Y. Z. You, C. Xu, Z. Y. Meng, and Z. Y. Lu, Phys. Rev. B **93**, 115150 (2016).
[30] P. Broecker and S. Trebst, Phys. Rev. B **94**, 075144 (2016).
[31] Z. X. Li, Y. F. Jiang, S. K. Jian, and H. Yao, Nat. Commun. **8**, 314 (2017).
[32] S. Gazit, M. Randeria, and A. Vishwanath, Nat. Phys. **13**, 484 (2017).
[33] Z. X. Li, Y. F. Jiang, and H. Yao, Phys. Rev. Lett. **119**, 107202 (2017).
[34] Z. X. Li, F. Wang, H. Yao, and D. H. Lee, Phys. Rev. B **95**, 214505 (2017).
[35] M. Bercx, J. S. Hofmann, F. F. Assaad, and T. C. Lang, Phys. Rev. B **95**, 035108 (2017).
[36] Y. Q. Qin, Y. Y. He, Y. Z. You, Z. Y. Lu, A. Sen, A. W. Sandvik, C. Xu, and Z. Y. Meng, Phys. Rev. X **7**, 031052 (2017).
[37] Z. X. Li, A. Vaezi, C. B. Mendl, and H. Yao, Sci. Adv. **4**, eaau1463 (2018).
[38] I. Esterlis, B. Nosarzewski, E. W. Huang, B. Moritz, T. P. Devereaux, D. J. Scalapino, and S. A. Kivelson, Phys. Rev. B **97**, 140501(R) (2018).
[39] S. Gazit, F. F. Assaad, S. Sachdev, A. Vishwanath, and C. Wang, Proc. Natl. Acad. Sci. USA **115**, E6987 (2018).
[40] I. Esterlis, S. A. Kivelson, and D. J. Scalapino, Phys. Rev. B **99**, 174516 (2019).
[41] Y. X. Zhang, W. T. Chiu, N. C. Costa, G. G. Batrouni, and R. T. Scalettar, Phys. Rev. Lett. **122**, 077602 (2019).
[42] X. Y. Xu, Y. Qi, L. Zhang, F. F. Assaad, C. Xu, and Z. Y. Meng, Phys. Rev. X **9**, 021022 (2019).

[43] T. C. Lang and A. M. Läuchli, Phys. Rev. Lett. **123**, 137602 (2019).
[44] Z.-X. Li, S.-K. Jian, and H. Yao, arXiv:1904.10975.
[45] Z.-X. Li, M. L. Cohen, and D.-H. Lee, Phys. Rev. B **100**, 245105 (2019).
[46] E. Berg, S. Lederer, Y. Schattner, and S. Trebst, Annu. Rev. Condens. Matter Phys. **10**, 63 (2019).
[47] N. C. Costa, K. Seki, S. Yunoki, and S. Sorella, Commun. Phys. **3**, 80 (2020).
[48] T. Sato, M. Hohenadler, T. Grover, J. McGreevy, and F. F. Assaad, Phys. Rev. B **104**, L161105 (2021).
[49] X. Y. Xu and T. Grover, Phys. Rev. Lett. **126**, 217002 (2021).
[50] C. Bauer, Y. Schattner, S. Trebst, and E. Berg, Phys. Rev. Res. **2**, 023008 (2020).
[51] Y. Otsuka, S. Yunoki, and S. Sorella, Phys. Rev. X **6**, 011029 (2016).
[52] Z. H. Liu, G. Pan, X. Y. Xu, K. Sun, and Z. Y. Meng, Proc. Natl. Acad. Sci. USA **116**, 16760 (2019).
[53] Y. Liu, W. Jiang, A. Klein, Y. Wang, K. Sun, A. V. Chubukov, and Z. Y. Meng, Phys. Rev. B **105**, L041111 (2022).
[54] M. Troyer and U. J. Wiese, Phys. Rev. Lett. **94**, 170201 (2005).
[55] M. B. Hastings, J. Math. Phys. **57**, 015210 (2016).
[56] Z. Ringel and D. L. Kovrizhin, Sci. Adv. **3**, e1701758 (2017).
[57] O. Golan, A. Smith, and Z. Ringel, Phys. Rev. Res. **2**, 043032 (2020).
[58] A. Smith, O. Golan, and Z. Ringel, Phys. Rev. Res. **2**, 033515 (2020).
[59] H. Shinaoka, Y. Nomura, S. Biermann, M. Troyer, and P. Werner, Phys. Rev. B **92**, 195126 (2015).
[60] R. Levy and B. K. Clark, Phys. Rev. Lett. **126**, 216401 (2021).
[61] G. Torlai, J. Carrasquilla, M. T. Fishman, R. G. Melko, and M. P. A. Fisher, Phys. Rev. Res. **2**, 032060(R) (2020).
[62] D. Hangleiter, I. Roth, D. Nagaj, and J. Eisert, Sci. Adv. **6**, eabb8341 (2020).
[63] J. Klassen, M. Marvian, S. Piddock, M. Ioannou, I. Hen, and B. M. Terhal, SIAM J. Comput. **49**, 1332 (2020).
[64] M. Marvian, D. A. Lidar, and I. Hen, Nat. Commun. **10**, 1571 (2019).
[65] A. J. Kim, P. Werner, and R. Valentí, Phys. Rev. B **101**, 045108 (2020).
[66] M. Ulybyshev, C. Winterowd, and S. Zafeiropoulos, arXiv:1906.02726.
[67] M. Ulybyshev, C. Winterowd, and S. Zafeiropoulos, Phys. Rev. D **101**, 014508 (2020).
[68] A. Alexandru, G. Başar, P. F. Bedaque, and N. C. Warrington, Rev. Mod. Phys. **94**, 015006 (2022).
[69] P. Broecker, J. Carrasquilla, R. G. Melko, and S. Trebst, Sci. Rep. **7**, 8823 (2017).
[70] J. Liu, H. Shen, Y. Qi, Z. Y. Meng, and L. Fu, Phys. Rev. B **95**, 241104(R) (2017).
[71] J.-L. Wynen, E. Berkowitz, S. Krieg, T. Luu, and J. Ostmeyer, Phys. Rev. B **103**, 125153 (2021).
[72] R. Blankenbecler, D. J. Scalapino, and R. L. Sugar, Phys. Rev. D **24**, 2278 (1981).
[73] J. E. Hirsch, Phys. Rev. B **28**, 4059 (1983).
[74] J. E. Hirsch, Phys. Rev. B **34**, 3216 (1986).
[75] G. M. Buendia, Phys. Rev. B **33**, 3519 (1986).
[76] G. G. Batrouni and P. de Forcrand, Phys. Rev. B **48**, 589 (1993).
[77] L. Chen and A.-M. Tremblay, Int. J. Mod. Phys. B **06**, 547 (1992).
[78] M. Bartholomew-Biggs, S. Brown, B. Christianson, and L. Dixon, J. Comput. Appl. Math. **124**, 171 (2000).
[79] A. G. Baydin, B. A. Pearlmutter, A. A. Radul, and J. M. Siskind, J. Mach. Learn. Res. **18**, 5595 (2017).
[80] C. C. Margossian, WIREs Data Min. Knowl. Discov. **9**, e1305 (2019).
[81] C. Hubig, arXiv:1907.13422.
[82] J.-G. Liu, L. Wang, and P. Zhang, Phys. Rev. Lett. **126**, 090506 (2021).
[83] J. Hasik, D. Poilblanc, and F. Becca, SciPost Phys. **10**, 012 (2021).
[84] L. Coopmans, D. Luo, G. Kells, B. K. Clark, and J. Carrasquilla, PRX Quantum **2**, 020332 (2021).
[85] K. Pakrouski, Quantum **4**, 315 (2020).
[86] B.-B. Chen, Y. Gao, Y.-B. Guo, Y. Liu, H.-H. Zhao, H.-J. Liao, L. Wang, T. Xiang, W. Li, and Z. Y. Xie, Phys. Rev. B **101**, 220409(R) (2020).
[87] S. Sorella and L. Capriotti, J. Chem. Phys. **133**, 234111 (2010).
[88] H. Xie, J. G. Liu, and L. Wang, Phys. Rev. B **101**, 245139 (2020).
[89] H. J. Liao, J. G. Liu, L. Wang, and T. Xiang, Phys. Rev. X **9**, 031041 (2019).
[90] S.-X. Zhang, Z.-Q. Wan, and H. Yao, arXiv:1911.09117.
[91] M. Hohenadler, Z. Y. Meng, T. C. Lang, S. Wessel, A. Muramatsu, and F. F. Assaad, Phys. Rev. B **85**, 115132 (2012).
[92] H. F. Trotter, Proc. Am. Math. Soc. **10**, 545 (1959).
[93] M. Suzuki, Prog. Theor. Phys. **56**, 1454 (1976).
[94] S. Beyl, F. Goth, and F. F. Assaad, Phys. Rev. B **97**, 085144 (2018).
[95] See Supplemental Material at http://link.aps.org/supplemental/10.1103/PhysRevB.106.L241109 for details, including the following: (1) a brief introduction to automatic differentiation, (2) the detailed algorithm for calculating gradients of the sign using AD, (3) a proof of sign-problem-free points in the Rashba-Hubbard model, (4) complementary QMC results of the sign-free Rashba-Hubbard model at $\lambda_R/t = \sqrt{2}$, (5) examples of parametrized HS transformations, and (6) complementary results for different λ_R.
[96] R. J. Willia, Mach. Learn. **8**, 229 (1992).
[97] J. P. Kleijnen and R. Y. Rubinstein, Eur. J. Oper. Res. **88**, 413 (1996).
[98] Y. A. Bychkov and E. I. Rashba, J. Phys. C: Solid State Phys. **17**, 6039 (1984).
[99] Y. S. Dedkov, M. Fonin, U. Rüdiger, and C. Laubschat, Phys. Rev. Lett. **100**, 107602 (2008).
[100] D. Marchenko, A. Varykhalov, M. R. Scholz, G. Bihlmayer, E. I. Rashba, A. Rybkin, A. M. Shikin, and O. Rader, Nat. Commun. **3**, 1232 (2012).
[101] J. Houdayer and A. K. Hartmann, Phys. Rev. B **70**, 014418 (2004).
[102] O. Melchert, arXiv:0910.5403.
[103] I. F. Herbut, Phys. Rev. Lett. **97**, 146401 (2006).